The morphology of high frequency oscillations (HFO) does not improve delineating the epileptogenic zone

Burnos, Sergey ; Frauscher, Birgit ; Zelmann, Rina ; Haegelen, Claire ; Sarnthein, Johannes ; Gotman, Jean

Abstract: OBJECTIVE: We hypothesized that high frequency oscillations (HFOs) with irregular amplitude and frequency more specifically reflect epileptogenicity than HFOs with stable amplitude and frequency. METHODS: We developed a fully automatic algorithm to detect HFOs and classify them based on their morphology, with types defined according to regularity in amplitude and frequency: type 1 with regular amplitude and frequency; type 2 with irregular amplitude, which could result from filtering of sharp spikes; type 3 with irregular frequency; and type 4 with irregular amplitude and frequency. We investigated the association of different HFO types with the seizure onset zone (SOZ), resected area and surgical outcome. RESULTS: HFO rates of all types were significantly higher inside the SOZ than outside. HFO types 1 and 2 were strongly correlated to each other and showed the highest rates among all HFOs. Their occurrence was highly associated with the SOZ, resected area and surgical outcome. The automatic detection emulated visual markings with 93% true positives and 57% false detections. CONCLUSIONS: HFO types 1 and 2 similarly reflect epileptogenicity. SIGNIFICANCE: For clinical application, it may not be necessary to separate real HFOs from "false oscillations" produced by the filter effect of sharp spikes. Also for automatically detected HFOs, surgical outcome is better when locations with higher HFO rates are included in the resection.

DOI: https://doi.org/10.1016/j.clinph.2016.01.002

The morphology of high frequency oscillations (HFO) does not improve delineating the epileptogenic zone

Sergey Burnos[1,2,3], Birgit Frauscher[3], Rina Zelmann[3], Claire Haegelen[4], Johannes Sarnthein[1,2], Jean Gotman[3]

[1]Neurosurgery Department, University Hospital Zurich, Zurich, Switzerland
[2]Neuroscience Center, ETH and University of Zurich, Zurich, Switzerland
[3]Montreal Neurological Institute and Hospital, Montreal, Quebec, Canada
[4]MediCIS, INSERM, Faculté de Médecine, University of Rennes, Rennes, France

Corresponding author:
Sergey Burnos
Klinik für Neurochirurgie, UniversitätsSpital Zürich,
8091 Zürich, Switzerland
sergey.burnos@usz.ch
Tel +41 44 255 2427

ABSTRACT

Objective:

We hypothesized that high frequency oscillations (HFOs) with irregular amplitude and frequency more specifically reflect epileptogenicity than HFOs with stable amplitude and frequency.

Methods:

We developed a fully automatic algorithm to detect HFOs and classify them based on their morphology, with types defined according to regularity in amplitude and frequency: type 1 with regular amplitude and frequency; type 2 with irregular amplitude, which could result from filtering of sharp spikes; type 3 with irregular frequency; and type 4 with irregular amplitude and frequency. We investigated the association of different HFO types with the seizure onset zone (SOZ), resected area and surgical outcome.

Results:

HFO rates of all types were significantly higher inside the SOZ than outside. HFO types 1 and 2 were strongly correlated to each other and showed the highest rates among all HFOs. Their occurrence was highly associated with the SOZ, resected area and surgical outcome. The automatic detection emulated visual markings with 93% true positives and 57% false detections.

Conclusions:

HFO types 1 and 2 similarly reflect epileptogenicity.

Significance:

For clinical application, it may not be necessary to separate real HFOs from “false oscillations” produced by the filter effect of sharp spikes. Also for automatically detected HFOs, surgical outcome is better when locations with higher HFO rates are included in the resection.

Keywords:
HFO; iEEG; epilepsy; ripple; filter effect; sharp spike

HIGHLIGHTS

- We developed a fully automatic algorithm to detect and classify HFOs based on their morphological appearance
- Epileptogenicity is similarly reflected by HFOs with regular and HFOs with irregular amplitude
- It seems not to be necessary to separate real HFOs from “false oscillations” produced by the filter effect of sharp spikes

1. INTRODUCTION

In many patients with therapy-refractory focal epilepsy, surgical resection of the epileptogenic zone represents the therapeutic option of choice. Currently, the identification of the seizure onset zone (SOZ) is used for delineating the epileptogenic zone (Rosenow and Lüders, 2001). Over the last years, high frequency oscillations (HFOs) have been proposed as a novel indicatorfor the epileptogenic zone (Jacobs et al., 2012; Urrestarazu et al., 2007; Zijlmans et al., 2012). HFOs are defined as spontaneous EEG patterns in the frequency range between 80-500 Hz, consisting of at least four oscillations that clearly stand out of the background activity (Jacobs et al., 2012). Interictal HFOs proved to be more specific in localizing the SOZ than spikes (Jacobs et al., 2008) and have shown a good correlation with the postsurgical outcome in epilepsy patients (Akiyama et al., 2011; Jacobs et al., 2010; van 't Klooster et al., 2015; Wu et al., 2010).

HFOs are differentiated into “ripples” (80-250 Hz) and “fast ripples” (FRs, 250-500 Hz) (Bragin et al., 1999). FRs are considered more specific for epileptogenicity because of their close relation to the SOZ (Engel et al., 2009). Ripples were shown to be a less specific marker of the epileptogenic zone than FRs regarding the surgical outcome (Akiyama et al., 2011; van 't Klooster et al., 2015). This is best explained by the fact that there are not only epileptic and hence pathological ripples, but also spontaneous physiological ripples generated by the healthy brain. It was shown that the hippocampus generates ripples associated with memory consolidation during sleep and rest (Girardeau and Zugaro, 2011). Spontaneous ripples were additionally found in the human visual cortex and the paracentral areas (Nagasawa et al., 2012; Wang et al., 2013).There are several reports of HFO induction in the human visual cortex (Kucewicz et al., 2014; Matsumoto et al., 2013), the auditory cortex (Edwards et al., 2005), the motor cortex (Darvas et al., 2010) and the language areas (Sinai et al., 2005). Event-related FRs can be recorded in humans during median nerve stimulation (Maegaki et al., 2000) or during cognitive processing (Kucewicz et al., 2014). Consequently, most clinical studies on ripples probably analyzed a mixture of physiological and pathological HFOs. Moreover, usually only the rates of HFOs are considered important for localizing epileptogenic areas.

There are several reports on the separation of pathological and physiological HFOs. Matsumoto et al. (2013) recorded event-related physiological HFOs in specific neocortical areas, induced by sensory stimulation or by motor tasks and compared them with spontaneous presumably pathological HFOs recorded from the SOZ. The authors parameterized each HFO according to the spectral amplitude, frequency and duration and then classified both types of HFOs using these parameters with a support vector machine. Pathological HFOs in the SOZ were highly distinguishable from physiologically-induced HFOs in the defined feature space. Although the data provided a statistical difference between the two groups of HFO, they did not assist in the classification of an individual HFO because of the large overlap between the groups.

Another approach based on the association of HFOs with slow waves during sleep is presented in Frauscher et al. (2015). Frauscher and co-authors showed an increased facilitation of epileptic HFOs during high amplitude slow waves. Interestingly, they found that HFOs inside the SOZ coupled differently to the slow wave than HFOs in presumably normal channels. This difference in coupling was confirmed in a recent study in 45 patients (Von Ellenrieder et al., in submission).

One possible approach to separate pathological and physiological HFOs would be to consider the different types of HFOs. Wang et al. (2013) classified ripples according to their presence with interictal epileptiform discharges (IED). The authors hypothesized that because IEDs are not normal physiologic events, HFOs occurring simultaneously with IEDs are assumed to be more specific for epileptogenicity. The authors showed that ripples superimposed on IEDs precisely marked the SOZ. In contrast, ripples independent of IEDs did not correlate with the SOZ.

Another approach based on the background activity was presented in Kerber et al. (2014) . The authors showed that resection of areas with ripples occurring in a flat background activity correlates with a good postsurgical outcome, whereas resection of areas generating ripples in a continuously oscillating background did not show an association with the surgical outcome.

Melani et al. (2013) investigated continuous high frequency activity in the ripple band. They observed this high frequency activity in channels outside the SOZ or a lesion, most exclusively in the hippocampus and occipital cortex. The authors concluded that the high

frequency activity they had described is of physiological nature and independent of epileptogenicity.

In this study we aimed 1) to define different types of HFOs based on their morphological appearance, and 2) to investigate whether the respective types have a different association with the SOZ, resected area and surgical outcome. We hypothesized that HFOs with irregular amplitude and frequency might more specifically reflect epileptogenicity than HFOs with stable amplitude and frequency. This reflects our clinical experience where we see regular HFOs also in physiological areas and irregular HFOs co-occur with spikes or with FRs, which are associated with pathological areas. To perform this analysis in a standardized way, we developed a fully automatic algorithm to detect and classify HFOs.

2. PATIENTS AND METHODS

2.1 Patient datasets

We used three different datasets. Table 1 describes each dataset in detail.

Dataset 1 was used to define different types of HFOs based on their morphological appearance. This dataset only consisted of channels inside the SOZ of 20 patients with medically intractable uni- or bilateral mesiotemporal lobe epilepsy, who underwent depth electrode implantation (electrodes either manufactured on site (9 contacts, 0.5 - 1 mm in length and separated by 5 mm) or commercially available (5 - 18 contacts, 2 mm in length, separated by 1.5 mm, DIXI Medical, France)) at the Montreal Neurological Institute and Hospital. The intracranial EEG (iEEG) was recorded with the Harmonie EEG system (Stellate, Montreal, Canada), with a low-pass filter of 500 Hz and a sampling rate of 2000 Hz. For each patient, a five-minute NREM sleep segment in one channel located in the SOZ was analyzed (Frauscher et al., in preparation).

Dataset 2 was used for the validation of the automatic HFO detector. This dataset was used before for the comparison of different HFO detectors (Zelmann et al., 2012). Nineteen patients with intractable epilepsy were implanted and recorded in the same way as Dataset 1. The Dataset 2 consisted of 19 one-minute sections, each with 10-39 channels, for a total of 373 channels. This dataset includes channels from inside and outside of the SOZ.

Dataset 3 was used for investigating whether the different HFO types have a specific association with the SOZ, resected area and surgical outcome. This dataset was used before for evaluating the impact of removing HFO-generating tissue on surgical outcome (Haegelen et al., 2013). Thirty patients with intractable epilepsy were implanted and recorded in the same way as Datasets 1 and 2. Information about the SOZ, resected area and surgical outcome (with a postoperative follow-up of at least 9 months) was known. The dataset 3 consisted of 1355 channels, from which 248 were in the SOZ (1107 outside) and 347 in the resected area (1008 outside). We analyzed intervals of iEEG of five-minute length. According to the International League Against Epilepsy (ILAE) classification

(Wieser et al., 2001), 15 patients had a good outcome (ILAE 1-3), and 15 had a poor outcome (ILAE 4-6).

Regarding the patient groups, there is a partial overlap between Datasets 1-3. We used recordings from total of 50 patients, and 15 of them were used more than once. Surgical decision was based on clinical information in combination with results of neuroimaging, identified SOZ in iEEG investigation and presence of eloquent cortex. Rates of interictal HFOs were not considered in the decision making process.

2.2 Visual definition of types of HFOs

The visual marking of HFOs was performed in the Stellate viewer by splitting the screen vertically, resulting in raw iEEG on the left side and 80 Hz high-pass filtered iEEG on the right side of the screen with time resolution of 0.6 sec across the monitor. For the marking, the filtered signal on the right side was considered, the unfiltered signal on the left served only for the differentiation from artifacts. Different from the original analysis (Jacobs et al., 2009), we visualized only one channel.

The detected HFOs were then visually reviewed by three experts (SB, BF, JG) on Dataset 1. Visual analysis based on regularity in amplitude and frequency of the filtered signal >80 Hz revealed four different types of HFO (Figure 1, Supplementary Figure S1).

Type 1 HFOs (Figure 1, panel (1 A-C)) are regular HFOs, with regular amplitude and frequency (Figure 1, panel (1 B)).

Type 2 HFOs (Figure 1, panel (2, 3 A-C)) are HFOs with irregular amplitude and one outstanding peak and with regular frequency (Figure 1, panel (2,3 B). After visual review of raw data, we assumed that this peak could be a result of filtering of the sharp components of the IED (Benar et al., 2010) (Figure 1 panel 2 A-C), but it could also reflect true ripple activity. Type 2 HFOs do not necessary co-occur with an IED (Figure 1 panel 3 A-C).

Type 3 HFOs (Figure 1, panel (4 A-C)) are HFOs with regular amplitude but irregular frequency (Figure 1, panel (4 B)). After visual review of filtered (>80 Hz) data, we observed ripples with varying frequency (Figure 1, panel 4 B). Many HFOs of this type have components in a wide frequency range, i.e. ripple and FR (Figure 1, panel 4 C) co-occurrence. This latter type is also in line with the literature where it was shown that the

majority of FRs (68-91%) is superimposed with ripples (Urrestarazu et al., 2007; Wang et al., 2013).

Type 4 HFOs (Figure 1, panel (5 A-C)) are HFOs with irregular amplitude and frequency (Figure 1, panel (5 B). This type is a combination of type 2 HFO and a FR. Type 4 HFOs can be a wide-frequency (80-500Hz) filtering effect of a sharp component of an IED.

Because of the previous clinical experience, we hypothesized that type 1 HFOs with regular amplitude and frequency was more physiological, as we observed them also in physiological areas (Nagasawa et al., 2012). Additionally, type 2 HFOs with irregular amplitude often co-occurred with spikes and, because of the spike pathological nature, we expected type 2 HFOs to be more pathological (Wang et al., 2013). Type 3 and type 4 HFOs included a FR, which was shown to be a very specific indicator of epileptogenicity (van 't Klooster et al., 2015). Therefore, types 3 and 4 HFOs were thought to be associated with pathological activity.

2.3 Automatic detector

In the automatic detection stage, we detected events in a similar way as the visual reviewer. We adapted the automatic detector from (Burnos et al., 2014) and used Dataset 2 with 373 channels for training and testing the detector. Similar to (Zelmann et al., 2012), we randomly chose 20% (76) of channels for training, resulting in 297 channels for evaluating the detector performance. The automatic detector consists of two steps – the baseline detector and the detector of HFOs.

2.3.1 Band-pass filters

The automatic detector separately identified ripples and FRs. For the detection of ripples, the iEEG was band-pass filtered (80-250 Hz) using a FIR equiripple filter (fStop1 = 70 Hz, fPass1 = 80Hz, fPass2 = 240 Hz, fStop2 = 250 Hz, stopband attenuation = -60 dB). For the detection of FRs, the iEEG was band-pass filtered (250-500 Hz) using a FIR

equiripple filter (fStop1 = 240 Hz, fPass1 = 250Hz, fPass2 = 490 Hz, fStop2 = 500 Hz, stopband attenuation = -60 dB).

2.3.2 Baseline detection

We defined the baseline as segments of iEEG with no oscillatory activity of any kind. The baseline detector is similar to (Zelmann et al., 2010), which is based on wavelet entropy (Rosso et al., 2001). We used entropy based on the Stockwell-transform (Stockwell et al., 1996), which measures the degree of randomness (vs. oscillatory activity) in the signal. The maximum theoretical Stockwell entropy (SE_{max}) is obtained for white noise, when contributions at all frequency ranges are equal. We considered a segment as a baseline (i.e. no oscillation present) when the Stockwell entropy was larger than 90% of the SE_{max}.

2.3.3 HFO detection

In the step of HFO detection, we detected HFOs based on the amplitude of the filtered signal. We calculated the envelope using the Hilbert transform (Burnos et al., 2014; Crepon et al., 2010). An event was marked when the envelope exceeded a threshold (Gardner et al., 2007; Staba et al., 2002). The threshold was defined as a percentile of the cumulative distribution of the amplitude of the Hilbert envelope taken for baseline segments (ThrHilbEnv, same for ripple and FR detection). This and the following procedure is different from (Burnos et al., 2014).The duration of the event was defined as the interval between upward and downward crossing of 0.5*threshold. If its duration exceeded 20 ms for ripples and 10 ms for FRs, this event was qualified as an HFO. We merged HFOs with an inter-event-interval of less than 10 ms into one single HFO. HFOs not having a minimum of 6 consecutive peaks (band-passed signal rectified >0 V) greater than a threshold were rejected. The threshold was chosen at a percentile of the cumulative distribution of the band-passed signal for baseline segments (ThrFiltRipple and ThrFiltFR, different for ripple and FR detection).

2.3.4 Parameter optimization

The HFO detection step was optimized to maximize sensitivity with respect to visual markings. All detected HFOs outside of any visual marking were assumed as wrong detections. With respect to that, we followed (Zelmann et al., 2012) and calculated the True Positive Rate (TPR) as the number of HFOs detected visually and automatically divided by the total number of visually detected HFOs. We calculated the False Detection Rate (FDR) as the number of automatically detected HFOs that are outside any visually marked HFO event divided by the total number of automatically detected HFOs. We optimized three thresholds ThrHilbEnv, ThrFiltRipple and ThrFiltFR.

Receiver operating characteristic (ROC) curves measure the performance of the detector when varying these three thresholds and were used for the evaluation of the detector. The parameters, which gives the TPR=1 and FDR=0 (top left corner), represent the perfect decision maker.

2.4 Automatic HFO classifier

In the automatic classification stage, we separated detected HFOs into four types, similar to those defined for visual review.

We checked the HFO for irregularity in amplitude. We compared the global maximum of the filtered HFO event (>80 Hz) to the nearest local maxima. We defined the ratio between global and local maxima as the threshold to differentiate type 1 HFOs with regular amplitude and type 2 HFOs with irregular amplitude. After training, the optimum threshold was set to 2.

In order to assess irregularity in frequency, we checked if an automatically detected FR occurred in the time interval of the HFO. We defined type 3 HFOs as HFOs occurring simultaneously with a FR.

An HFO with both irregular amplitude and frequency was classified as type 4.

For the training of the classifier, we used 5 patients from Dataset 1. We used another 15 patients from Dataset 1 for validation of the classifier. The first 50 HFOs in each patient were visually classified by an expert (BF), who was blind to the automatic classification

results. In three patients we identified only 29, 32 and 41 HFOs in the 5-minute recordings. The agreement between the viewer and the classifier was calculated based on the four types of HFOs.

2.5 Analysis of Dataset 3

We finally applied the optimized automatic detector and classifier on Dataset 3. We calculated the rates of HFOs together with rates of HFOs of each type for all channels. We compared rates of HFOs of each type in channels inside and outside the SOZ and the resected area. Additionally, we tested whether the surgical resection of channels carrying HFOs of each type was correlated with a good postsurgical outcome and, conversely, whether a non-resection of the HFO channels resulted in poor postsurgical outcome. If not stated otherwise, the rates are presented in median [range] HFOs/min.

2.6 Statistical analysis

We used the Wilcoxon rank sum test to compare rates of HFOs of each type in channels inside versus outside the SOZ and in channels inside versus outside the resected area. We also calculated the ratio between rates of HFOs of each type in resected (Res) and non-resected (nonRes) channels, using the following formula (Haegelen et al., 2013):

$$[\bar{R}_{ev}(Res) - \bar{R}_{ev}(nonRes)]/[\bar{R}_{ev}(Res) + \bar{R}_{ev}(nonRes)],$$

where $\bar{R}$ is the mean rate of an event (ev, HFO type 1-4). A ratio of +1 indicates that the HFO generating areas have been completely resected. A ratio of -1 indicates that no HFO generating area has been resected.

We used the Wilcoxon rank sum test to compare the ratios of events between patients with a good and poor outcome. We expect that ratios would be close to +1 in patients with a good outcome and close to -1 in patients with a poor outcome The Spearman's rho was used to explore correlations between rates of HFOs of different types in channels inside the SOZ. Statistical significance was established for $p<0.05$. All statistics were corrected for multiple comparisons by the Bonferroni-Holm method.

3. RESULTS

3.1 Accuracy of the detector

The accuracy of the detector in emulating visual marking was determined in Dataset 2. We used this dataset because it was already used to compare different HFO detectors (Zelmann et al., 2012). With optimal parameter settings we obtained TPR = 77±30% and FDR = 28±27%, which were closest to the left top corner of the ROC-plot. However, we preferred to choose parameters such that TPR = 93±15% [95% confidence interval 91-95%] and FDR = 58±27% [55-60%], so that the TPR was comparable to the MNI detector (Zelmann et al., 2012) and more events were available for subsequent analysis.

The visual and the automatic classification into HFO types agreed well, with an inter-rater reliability of mean 79%, median [range] 82% [54-96]% in Dataset 1 (N=15 patients).

3.2 HFO types and the SOZ

Dataset 3 has been used previously to evaluate the impact of removing the HFO-generating tissue on surgical outcome (Haegelen et al., 2013). We aimed to replicate this analysis by the automatic detection and by differentiating between HFO types. In Dataset 3 we found 115884 HFOs, from which 85525 (74%) were type 1 HFOs, 20074 (17%) type 2 HFOs, 2969 (3%) type 3 HFOs and 7316 (6%) type 4 HFOs. When analyzing all HFOs together, the rates were significantly higher inside the SOZ than outside the SOZ: 25.6 [0–204.4] vs. 2.8 [0-191.6] HFOs/min, $p<0.001$.

In the separate analysis of HFO types (Figure 2), the rates of HFO of each type were significantly higher inside the SOZ than outside the SOZ. For type 1 HFOs, rates were 17.7 [0-187.4] vs. 2 [0-173.4] HFOs/min; type 2 – 3.9 [0-63] vs. 0.2 [0-55] HFOs/min; type 3 – 0.4 [0-18.4] vs. 0 [0-9] HFOs/min; and type 4 – 0.4 [0-27.2] vs. 0 [0-53.8] HFOs/min; all $p<0.001$. The rates of type 3 and type 4 HFOs were very low and we excluded these two HFO types from further analysis.

Additionally, we calculated the correlation between rates of different HFO types across channels inside the SOZ. Figure 3 shows the correlation between rates of HFOs types 1 and 2 across channels in the SOZ. We found a high correlation between all HFO types (correlation type 1 and type 2 – Spearman's rho=0.85; type 1-3 rho=0.69; type 1-4 rho=0.55; type 2-3 rho=0.74; type 2-4 rho=0.69; type 3-4 rho=0.84, all p<0.001). For illustration see Table 2 and Supplementary Figure 1.

3.3 HFO types and the surgical resection

Figure 4 shows results of the comparison of HFOs rates of each type against the resected area in Dataset 3. When analyzing all HFOs together, the rates were significantly higher inside the resected area than outside: 7 [0–158.4] *vs.* 3.6 [0-204.4] HFOs/min, p<0.001.

Also in the separate analysis of HFO types, the rates of HFO of each type were significantly higher inside the resected area than outside. For type 1 HFOs, rates were 5 [0-127.6] *vs.* 2.6 [0-187.4] HFOs/min, p<0.001. For type 2 HFOs, rates were 0.8 [0-51.4] *vs.* 0.4 [0-63] HFOs/min, p<0.001.

3.4 HFOs and the surgical outcome

Figure 5 shows results of the comparison of the ratio of HFO rates of each type against the surgical outcome in Dataset 3. We found that the ratio between HFO rates in resected and non-resected channels was significantly higher in patients with a good outcome (ILAE classes 1-3) compared to patients with a poor outcome (ILAE classes 4-6) (median [range]: 0.3 [-0.8 – 1] *vs.* 0.0 [-1 – 0.3], p=0.016, after the Bonferroni-Holm correction).

When subdividing the analysis by HFO types, results were marginally significant with the Bonferroni-Holms correction (p=0.056) and were significant if we did not do the Bonferroni-Holm correction, which is how most other studies have been done. The ratio between HFO rates in resected and non-resected channels was significantly higher in patients with a good outcome than in patients with a poor outcome for type 1 HFOs (median [range]: 0.1 [-0.8 – 1] *vs.* -0.1 [-1 – 0.3], p=0.028), and for type 2 HFOs: 0.4 [-1 –

1] *vs.* 0.0 [-1 – 0.4] (p=0.031). There was thus no difference with respect to outcome between type 1 and type 2 HFOs.

4. DISCUSSION

Our classification of HFOs according to their morphology showed that all four HFO types reflect epileptogenicity equally well since all types of HFO are highly associated with the SOZ. We could also show that the most frequently occurring HFO types (1 and 2) are associated with the resected area and the surgical outcome.

In our fully automatic application on Dataset 3, we found that rates of HFOs were higher inside the SOZ, and resection of areas with higher HFO rates predicted good surgical outcome. These two results agree with results obtained with the visual marking reported in the same dataset (Haegelen et al., 2013).

4.1 Properties of the four HFO types

Type 1 HFOs were by far the most frequent (74% of all HFOs in Dataset 3). Because their amplitude and frequency is very regular, we had initially hypothesized that type 1 HFOs are less specific for epileptogenicity. This hypothesis was not confirmed, since all four HFO types predicted outcome equally well. We now consider that type 1 HFOs can be found in both pathological as well as physiological conditions, albeit the rate is much higher in the epileptogenic zone compared to the normal zone.

Type 2 HFOs represented 17% of all HFOs. The visual and automatic detection of this HFO type is challenging, because its irregular amplitude could be either an effect of filtering sharp epileptiform spikes (“false ripple”, (Benar et al., 2010)) or a ripple superimposed on a sharp spike (Amiri et al., 2015). We showed that type 1 and type 2 HFO rates are highly correlated (Figure 3) and reflect epileptogenic activity equally well. We speculate that higher rates of the type 2 HFOs in the SOZ and resected area could result from high spike rates or from spike sharpness. It was shown in Hufnagel et al. (2000) that the shortest spike duration and the maximal spike frequency were highly associated with a zone ≤2 cm from the SOZ.

HFOs of type 3 and 4 are composed of both a ripple and a fast component resembling a FR (Figure 1). FRs in the post resection iEEG were good predictors of recurrent seizures (van 't Klooster et al., 2015). The broad frequency and amplitude range of type 4 HFO could result from artifacts. Since HFOs of type 3 and 4 only represent 9% of all HFOs, the predictive power of HFOs would remain favorable even if we exclude them from the analysis.

4.2 Association of HFOs with the SOZ, the resected area and the surgical outcome

All HFO types were strongly associated with the SOZ, even though the rates of type 3 and type 4 HFO were very low. High correlations between HFO types in SOZ channels support the fact that all HFO types carry similar information about epileptogenicity. Because of the low rates of HFO type 3 and type 4 we used only type 1 and type 2 HFO for the analysis of HFO rates in the resected area.

All HFOs together, and also type 1 and type 2 HFO separately, were strongly associated with the resected area. In extension of the analysis of (Haegelen et al., 2013), we found that rates of HFOs of each type were significantly higher in the resected area. This is an expected result as the resected area and the SOZ are closely overlapping.

Good surgical outcome was associated with the resection of channels with high rates of HFOs, using all HFOs of all types. This was significant also after applying the Bonferroni-Holm correction, which places a stricter requirement on statistical significance than most other publications on this topic.

In a separate analysis of type 1 and type 2 HFOs, association of good surgical outcome with the resection of channels with high rates of HFOs type 1 and type 2 were marginally significant ($p=0.056$) with the Bonferroni-Holm correction. The separate analysis was significant without the Bonferroni-Holm correction, as it is done in most other publications on this topic. Given that the smaller number of events maybe the cause of this marginal significance, we conclude that there is a good chance that both types are good indicators for the epileptogenic zone.

4.3 Automatic detector

The automatic detector we presented here has several important features, which distinguish it from existing detectors. We used two different frequency ranges in order to detect separately ripples and FRs. The aim of our detector was to detect only visually marked events and to have the least possible number of false detections. In comparison to the MNI detector (Zelmann et al., 2012), which has the best performance among several existing detectors, our detector has a slightly lower sensitivity (93% *vs.* 98%) and lower FDR (58% *vs.* 76%) in dataset 2.

How does the FDR affect our analysis in dataset 3, where there was no visual marking? Some of the “false” HFOs detected may represent pure epileptic spikes. It is true that the detector detects events in dataset 3 that may not have been marked by human interpreters, but these events are nevertheless classified according to the algorithm into the 4 categories and each has therefore the characteristics of one of the 4 HFO types. Detected HFOs will fall in type 2 if they have a good chance of resulting from spike filtering. Additionally, it has been shown that spikes inside the SOZ are sharper and shorter than outside (Hufnagel et al., 2000), which increases this chance. It may therefore be that the epileptogenic zone is strongly associated with true HFOs as well as with sharp spikes, which appear as “false” HFOs after filtering.

4.4 Other approaches to discriminate physiological and pathological HFOs

The approach we presented here is novel and different from the existing ones (Kerber et al., 2014; Wang et al., 2013) as it is based exclusively on the morphology of HFOs, and not based on relation to spikes or background activity. For more accurate comparison and delineation of pathological and physiological HFOs, one should compare rates of different HFO types of cortical tissue without epilepsy.

5. CONCUSIONS

All four HFO types are highly associated with the SOZ. The strong correlation between type 1 and type 2 HFOs together with their association with the SOZ, resected area and

surgical outcome show that both HFO types similarly reflect epileptogenic activity. The exclusion of HFO type 3 and 4 has probably no influence on the results, because of their low rates and similar association with the SOZ. For clinical application, it may not be necessary to separate real HFOs from “false oscillations” produced by the filter effect of sharp spikes since type 2 HFOs, which includes most such oscillations, have the same association with the epileptogenic zone as the more regular type 1 HFOs. The surgical outcome is better when locations with higher HFO rates are included in the resection. This standardized analysis relied on a newly developed and fully automated HFO detection method.

6. CONFLICT OF INTEREST STATEMENT

None.

7. ACKNOWLEDGEMENTS

We cordially thank Dr. Nicolas von Ellenrieder and Dr. Tommaso Fedele for fruitful discussions. Sergey Burnos was supported by the Laszlo and Etelka Kohler Brain@McGill Graduate/Postdoctoral Travel Award and by the Vontobel Stiftung, EMDO Stiftung and Herzog-Egli Stiftung. Birgit Frauscher was supported by the Austrian Science Funds (Schroedinger fellowship abroad J3485-B24). This research was supported by a grant from the Canadian Institutes of Health Research (MOP-102710).

7. BIBLIOGRAPHY

Akiyama, T., McCoy, B., Go, C.Y., Ochi, A., Elliott, I.M., Akiyama, M., Donner, E.J., Weiss, S.K., Snead, O.C., Rutka, J.T., Drake, J.M., Otsubo, H., 2011. Focal resection of fast ripples on extraoperative intracranial EEG improves seizure outcome in pediatric epilepsy. Epilepsia 52, 1802-1811.

Amiri, M., Lina, J.M., Pizzo, F., Gotman, J., 2015. High Frequency Oscillations and spikes: Separating real HFOs from false oscillations. Clin Neurophysiol.

Benar, C.G., Chauviere, L., Bartolomei, F., Wendling, F., 2010. Pitfalls of high-pass filtering for detecting epileptic oscillations: a technical note on "false" ripples. Clin Neurophysiol 121, 301-310.

Bragin, A., Engel, J., Wilson, C.L., Fried, I., Buzsaki, G., 1999. High-frequency oscillations in human brain. Hippocampus 9, 137-142.

Burnos, S., Hilfiker, P., Surucu, O., Scholkmann, F., Krayenbuhl, N., Grunwald, T., Sarnthein, J., 2014. Human intracranial high frequency oscillations (HFOs) detected by automatic time-frequency analysis. PLoS One 9, e94381.

Crepon, B., Navarro, V., Hasboun, D., Clemenceau, S., Martinerie, J., Baulac, M., Adam, C., Le Van Quyen, M., 2010. Mapping interictal oscillations greater than 200 Hz recorded with intracranial macroelectrodes in human epilepsy. Brain 133, 33-45.

Darvas, F., Scherer, R., Ojemann, J.G., Rao, R.P., Miller, K.J., Sorensen, L.B., 2010. High gamma mapping using EEG. Neuroimage 49, 930-938.

Edwards, E., Soltani, M., Deouell, L.Y., Berger, M.S., Knight, R.T., 2005. High gamma activity in response to deviant auditory stimuli recorded directly from human cortex. J Neurophysiol 94, 4269-4280.

Engel, J., Jr., Bragin, A., Staba, R., Mody, I., 2009. High-frequency oscillations: what is normal and what is not? Epilepsia 50, 598-604.

Frauscher, B., von Ellenrieder, N., Ferrari-Marinho, T., Avoli, M., Dubeau, F., Gotman, J., 2015. Facilitation of epileptic activity during sleep is mediated by high amplitude slow waves. Brain. The Author (2015). Published by Oxford University Press on behalf of the Guarantors of Brain., England, pp. 1629-1641.

Gardner, A.B., Worrell, G.A., Marsh, E., Dlugos, D., Litt, B., 2007. Human and automated detection of high-frequency oscillations in clinical intracranial EEG recordings. Clin Neurophysiol 118, 1134-1143.

Girardeau, G., Zugaro, M., 2011. Hippocampal ripples and memory consolidation. Curr Opin Neurobiol. 2011 Elsevier Ltd, England, pp. 452-459.

Haegelen, C., Perucca, P., Chatillon, C.E., Andrade-Valenca, L., Zelmann, R., Jacobs, J., Collins, D.L., Dubeau, F., Olivier, A., Gotman, J., 2013. High-frequency oscillations, extent of surgical resection, and surgical outcome in drug-resistant focal epilepsy. Epilepsia.

Hufnagel, A., Dumpelmann, M., Zentner, J., Schijns, O., Elger, C.E., 2000. Clinical relevance of quantified intracranial interictal spike activity in presurgical evaluation of epilepsy. Epilepsia 41, 467-478.

Jacobs, J., LeVan, P., Chander, R., Hall, J., Dubeau, F., Gotman, J., 2008. Interictal high-frequency oscillations (80-500 Hz) are an indicator of seizure onset areas independent of spikes in the human epileptic brain. Epilepsia 49, 1893-1907.

Jacobs, J., Levan, P., Chatillon, C.E., Olivier, A., Dubeau, F., Gotman, J., 2009. High frequency oscillations in intracranial EEGs mark epileptogenicity rather than lesion type. Brain 132, 1022-1037.

Jacobs, J., Staba, R., Asano, E., Otsubo, H., Wu, J.Y., Zijlmans, M., Mohamed, I., Kahane, P., Dubeau, F., Navarro, V., Gotman, J., 2012. High-frequency oscillations (HFOs) in clinical epilepsy. Prog Neurobiol 98, 302-315.

Jacobs, J., Zijlmans, M., Zelmann, R., Chatillon, C.E., Hall, J., Olivier, A., Dubeau, F., Gotman, J., 2010. High-frequency electroencephalographic oscillations correlate with outcome of epilepsy surgery. Ann Neurol 67, 209-220.

Kerber, K., Dumpelmann, M., Schelter, B., Le Van, P., Korinthenberg, R., Schulze-Bonhage, A., Jacobs, J., 2014. Differentiation of specific ripple patterns helps to identify epileptogenic areas for surgical procedures. Clin Neurophysiol 125, 1339-1345.

Kucewicz, M.T., Cimbalnik, J., Matsumoto, J.Y., Brinkmann, B.H., Bower, M.R., Vasoli, V., Sulc, V., Meyer, F., Marsh, W.R., Stead, S.M., Worrell, G.A., 2014. High frequency oscillations are associated with cognitive processing in human recognition memory. Brain 137, 2231-2244.

Maegaki, Y., Najm, I., Terada, K., Morris, H.H., Bingaman, W.E., Kohaya, N., Takenobu, A., Kadonaga, Y., Luders, H.O., 2000. Somatosensory evoked high-frequency oscillations recorded directly from the human cerebral cortex. Clin Neurophysiol 111, 1916-1926.
Matsumoto, A., Brinkmann, B.H., Matthew Stead, S., Matsumoto, J., Kucewicz, M.T., Marsh, W.R., Meyer, F., Worrell, G., 2013. Pathological and physiological high-frequency oscillations in focal human epilepsy. J Neurophysiol 110, 1958-1964.
Melani, F., Zelmann, R., Mari, F., Gotman, J., 2013. Continuous High Frequency Activity: A peculiar SEEG pattern related to specific brain regions. Clinical Neurophysiology 124, 1507-1516.
Nagasawa, T., Juhasz, C., Rothermel, R., Hoechstetter, K., Sood, S., Asano, E., 2012. Spontaneous and visually driven high-frequency oscillations in the occipital cortex: intracranial recording in epileptic patients. Hum Brain Mapp 33, 569-583.
Rosenow, F., Lüders, H., 2001. Presurgical evaluation of epilepsy. Brain 124, 1683-1700.
Rosso, O.A., Blanco, S., Yordanova, J., Kolev, V., Figliola, A., Schurmann, M., Basar, E., 2001. Wavelet entropy: a new tool for analysis of short duration brain electrical signals. J Neurosci Methods 105, 65-75.
Sinai, A., Bowers, C.W., Crainiceanu, C.M., Boatman, D., Gordon, B., Lesser, R.P., Lenz, F.A., Crone, N.E., 2005. Electrocorticographic high gamma activity versus electrical cortical stimulation mapping of naming. Brain 128, 1556-1570.
Staba, R.J., Wilson, C.L., Bragin, A., Fried, I., Engel, J., Jr., 2002. Quantitative analysis of high-frequency oscillations (80-500 Hz) recorded in human epileptic hippocampus and entorhinal cortex. J Neurophysiol 88, 1743-1752.
Stockwell, R.G., Mansinha, L., Lowe, R.P., 1996. Localization of the complex spectrum: the S transform. Signal Processing, IEEE Transactions on 44, 998-1001.
Urrestarazu, E., Chander, R., Dubeau, F., Gotman, J., 2007. Interictal high-frequency oscillations (100-500 Hz) in the intracerebral EEG of epileptic patients. Brain 130, 2354-2366.
van 't Klooster, M.A., van Klink, N.E., Leijten, F.S., Zelmann, R., Gebbink, T.A., Gosselaar, P.H., Braun, K.P., Huiskamp, G.J., Zijlmans, M., 2015. Residual fast ripples in the intraoperative corticogram predict epilepsy surgery outcome. Neurology 85, 120-128.
Wang, S., Wang, I.Z., Bulacio, J.C., Mosher, J.C., Gonzalez-Martinez, J., Alexopoulos, A.V., Najm, I.M., So, N.K., 2013. Ripple classification helps to localize the seizure-onset zone in neocortical epilepsy. Epilepsia 54, 370-376.
Wieser, H.G., Blume, W.T., Fish, D., Goldensohn, E., Hufnagel, A., King, D., Sperling, M.R., Luders, H., Pedley, T.A., 2001. ILAE Commission Report. Proposal for a new classification of outcome with respect to epileptic seizures following epilepsy surgery. Epilepsia 42, 282-286.
Wu, J.Y., Sankar, R., Lerner, J.T., Matsumoto, J.H., Vinters, H.V., Mathern, G.W., 2010. Removing interictal fast ripples on electrocorticography linked with seizure freedom in children. Neurology 75, 1686-1694.
Zelmann, R., Mari, F., Jacobs, J., Zijlmans, M., Chander, R., Gotman, J., 2010. Automatic detector of high frequency oscillations for human recordings with macroelectrodes. Conf Proc IEEE Eng Med Biol Soc 2010, 2329-2333.
Zelmann, R., Mari, F., Jacobs, J., Zijlmans, M., Dubeau, F., Gotman, J., 2012. A comparison between detectors of high frequency oscillations. Clin Neurophysiol 123, 106-116.
Zijlmans, M., Jiruska, P., Zelmann, R., Leijten, F.S., Jefferys, J.G., Gotman, J., 2012. High-frequency oscillations as a new biomarker in epilepsy. Ann Neurol 71, 169-178.

8. LEGENDS

Figure 1. Representative examples of the four HFO type.
(A) 0.3 sec epoch of a raw intracranial EEG bipolar channel. (B) High-pass (>80 Hz) filtered intracranial EEG of panel A. (C) High-pass (>250 Hz) filtered intracranial EEG of panel A. (1 A-C) Example of a type 1 HFO with regular amplitude and frequency. (2 A-C) Example of a type 2 HFO at the time of a spike. The irregular amplitude of the HFO could be due to a filter effect of the sharp spike. (3 A-C) Example of a type 2 HFO occurring independently of a spike. We observe an irregular amplitude HFO with one outstanding peak. Note that this peak is similar to that observed in the context of a spike. (4 A-C) Example of a type 3 HFO with irregular frequency, with activity in both frequency ranges (4B, 4C). (5 A-C) Example of a type 4 HFO, with irregular amplitude and irregular frequency.

Figure 2. Comparison of rates of the different HFO types against the SOZ. Boxplots illustrating rates of all HFOs in channels inside the seizure onset zone (SOZ, N=248) and outside (nonSOZ, N=1107). The rates of all HFOs together and the rates of the HFOs of each type were significantly higher inside the SOZ than outside. Rates of type 3 and 4 HFOs were much lower than those of type 1 and 2 HFOs.The red numbers present the number of outliers exceeding the maximum rate of the y-axis. The boxplots in right top corner repeat rates of types 3 and 4 HFO on a larger scale. *p≤0.05, **p≤0.001.

Figure 3. Correlation (Spearman's rho =0.85, p<0.001) between rates of type 1 and type 2 HFOs (red crosses) across channels inside the SOZ. The high correlation supports the fact that type 1 and 2 HFOs carry similar information about epileptogenicity. The black dashed line is the linear fit (slope = 2.9).

Figure 4. Comparison of rates of the different HFO types against surgical resection. Boxplots illustrating rates of all HFOs and types 1-2 HFO in channels inside the resected area (Res, N=347) and outside (nonRes, N=1008). The rates of all HFOs together and the rates of the HFOs of each type were significantly higher inside the resected area than outside. The red numbers present the number of outliers exceeding the maximum rate of the y-axis. *p≤0.05, **p≤0.001.

Figure 5. Comparison of ratio mean rates of the different HFO types against surgical outcome. Boxplots illustrating mean ratios of all HFOs and HFOs of types 1-2 in patients with good outcome (ILAE 1-3, N=15) and with poor outcome (ILAE 4-6, N=15). The ratio between HFO rates (all HFOs together, Type 1 HFO and Type 2 HFO) in resected and non-resected channels was significantly higher in patients with a good outcome than in patients with a poor outcome. Symbol (*) indicates a statistically significant difference with p≤0.05 after the Bonferroni-Holm correction for multiple comparisons. Symbol (+) indicates a statistically significant difference with p≤0.05 without the Bonferroni-Holm correction. A ratio of -1 signifies that all events were in non-resected areas, whereas a ratio of 1 signifies that all events were in resected areas. Ev event; R mean rate of event; Res resected channels; nonRes non-resected channels.

Supplementary Material.

Figure S1. Correlation between rates of different HFO types across channels inside the SOZ. The black dashed line is the linear fit. We found a high correlation between all HFO types. Correlation between type 1 and type 2 HFO – Spearman's rho=0.85; type 1-3 rho=0.69; type 1-4 rho=0.55; type 2-3 rho=0.74; type 2-4 rho=0.69; type 3-4 rho=0.84; all $p<0.001$.

Figure S2. Additional representative examples of the four HFO type.
(A) 0.3 sec epoch of a raw intracranial EEG bipolar channel. (B) High-pass (>80 Hz) filtered intracranial EEG of panel A. (C) High-pass (>250 Hz) filtered intracranial EEG of panel A. (1 A-C) Example of a type 1 HFO with regular amplitude and frequency. (2 A-C) Example of a type 2 HFO at the time of a spike. The irregular amplitude of the HFO could be due to a filter effect of the sharp spike. (3 A-C) Example of a type 2 HFO occurring independently of a spike. We observe an irregular amplitude HFO with one outstanding peak. Note that this peak is similar to that observed in the context of a spike. (4 A-C) Example of a type 3 HFO with irregular frequency, with activity in both frequency ranges (4B, 4C). (5 A-C) Example of a type 4 HFO, with irregular amplitude and irregular frequency.

9. TABLES

Dataset	N patient	N channels	Location	Reference
1	20	20	SOZ in mTLE	(Frauscher et al., in preparation)
2	19	373	TLE, ETLE	(Zelmann et al., 2012)
3	30	1355	29 TLE, 9 ETLE	(Haegelen et al., 2013)

Table 1. Information on the three datasets investigated in this study. SOZ seizure onset zone; ETLE extratemporal lobe epilepsy; mTLE mesial temporal lobe epilepsy; TLE temporal lobe epilepsy.

	Type 1 HFO	Type 2 HFO	Type 3 HFO	Type 4 HFO
Type 1 HFO	1	0.85	0.69	0.55
Type 2 HFO	–	1	0.74	0.69
Type 3 HFO	–	–	1	0.84
Type 4 HFO	–	–	–	1

Table 2. Correlation (Spearman's rho) between rates of the four HFO types across channels inside the SOZ. All $p<0.001$.

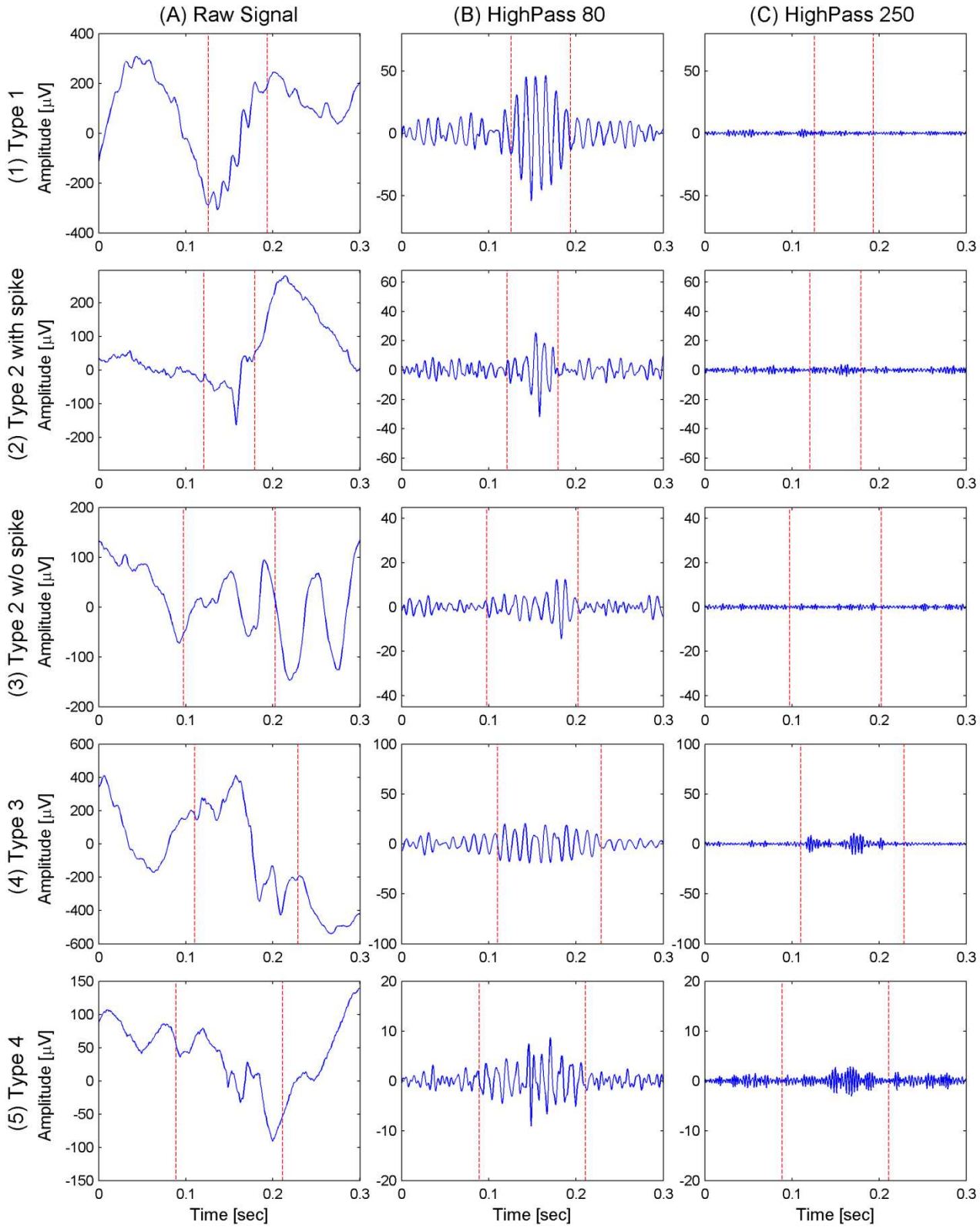
(A) Raw Signal
(B) HighPass 80
(C) HighPass 250
(1) Type 1
(2) Type 2 with spike
(3) Type 2 w/o spike
(4) Type 3
(5) Type 4
Amplitude [μV]
Time [sec]

Figure 1

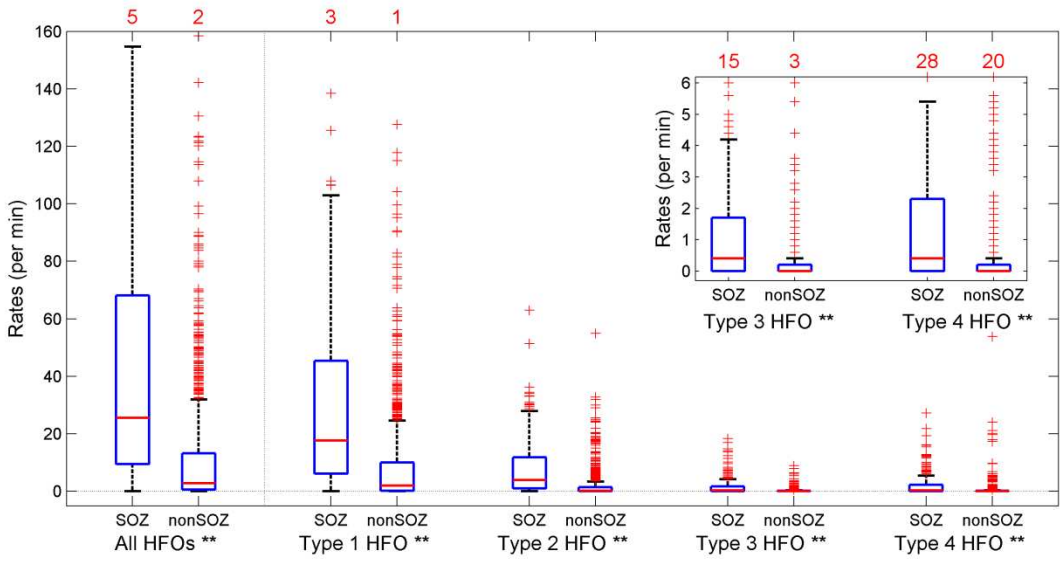

Figure 2

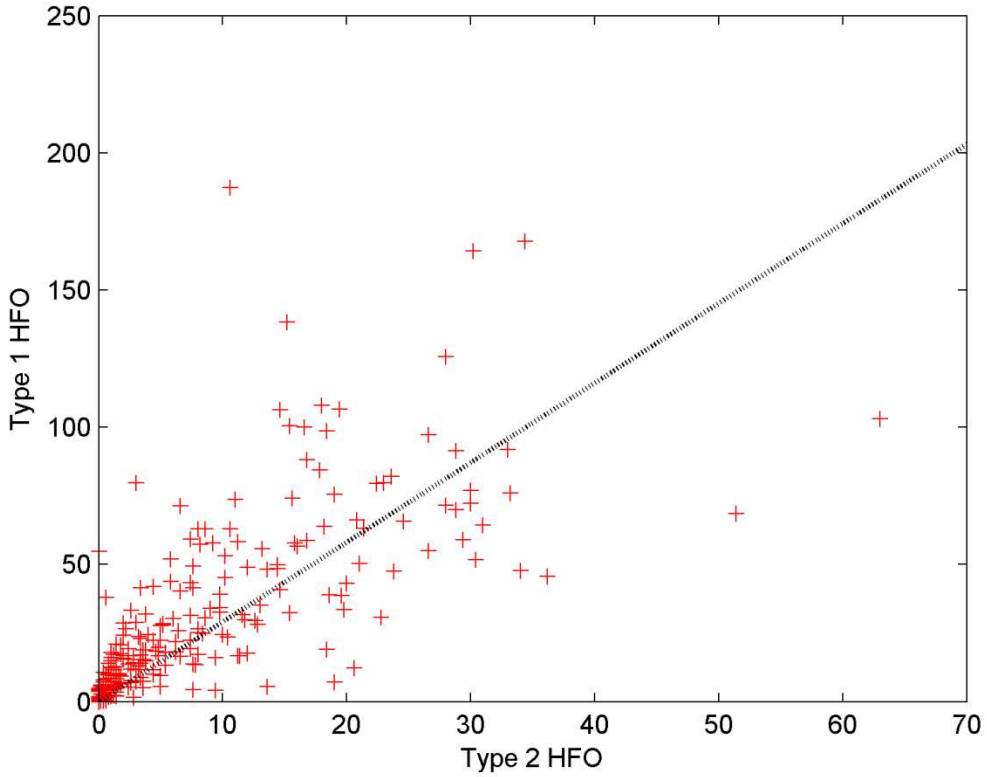

Figure 3

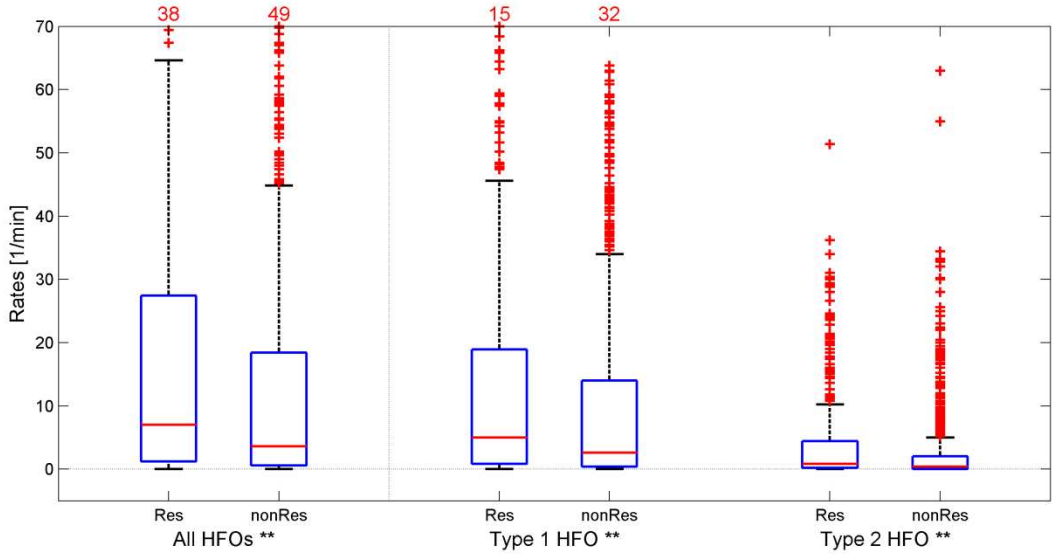

Figure 4

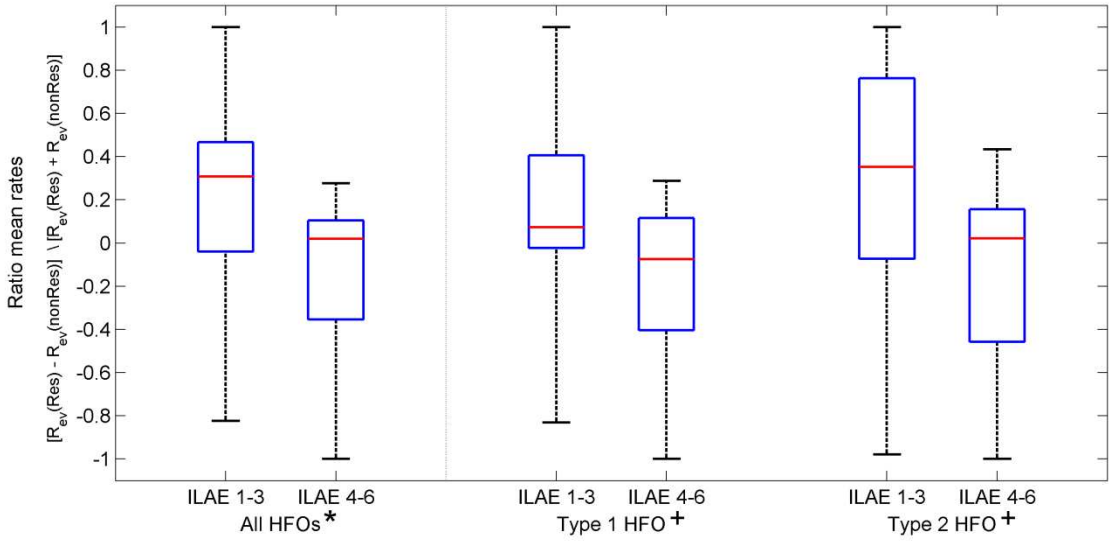

Figure 5

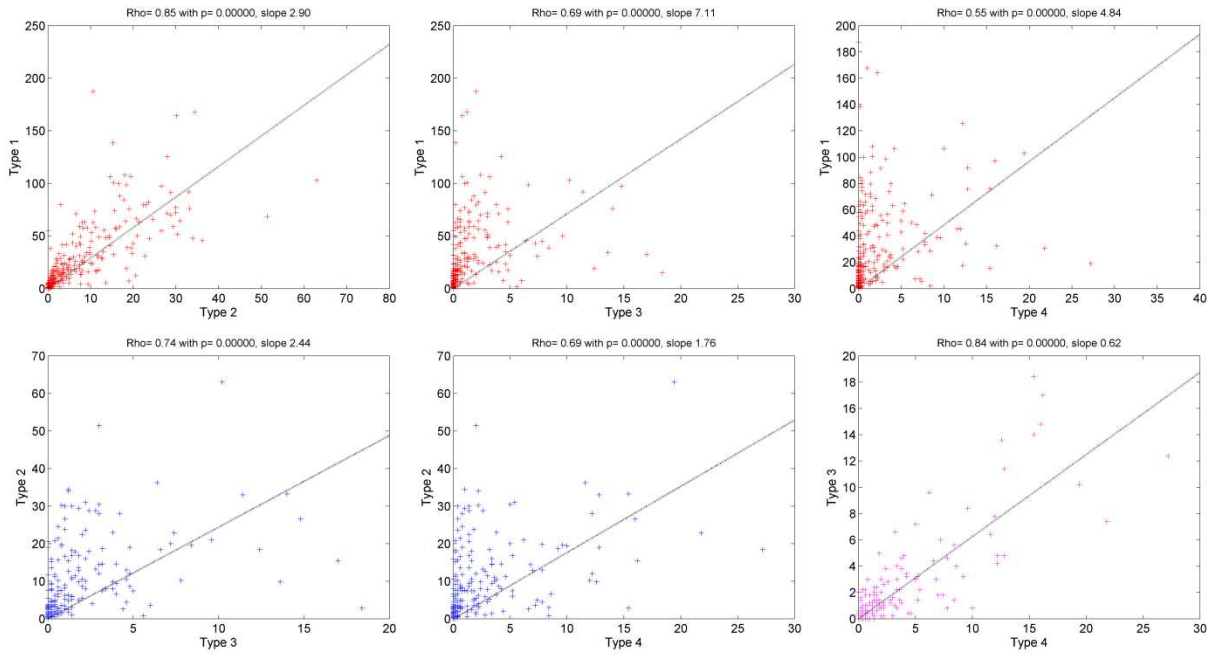
Rho= 0.85 with ρ= 0.00000, slope 2.90
Type 1
Type 2
Rho= 0.69 with ρ= 0.00000, slope 7.11
Type 1
Type 3
Rho= 0.55 with ρ= 0.00000, slope 4.84
Type 1
Type 4
Rho= 0.74 with ρ= 0.00000, slope 2.44
Type 2
Type 3
Rho= 0.69 with ρ= 0.00000, slope 1.76
Type 2
Type 4
Rho= 0.84 with ρ= 0.00000, slope 0.62
Type 3
Type 4

Figure S1

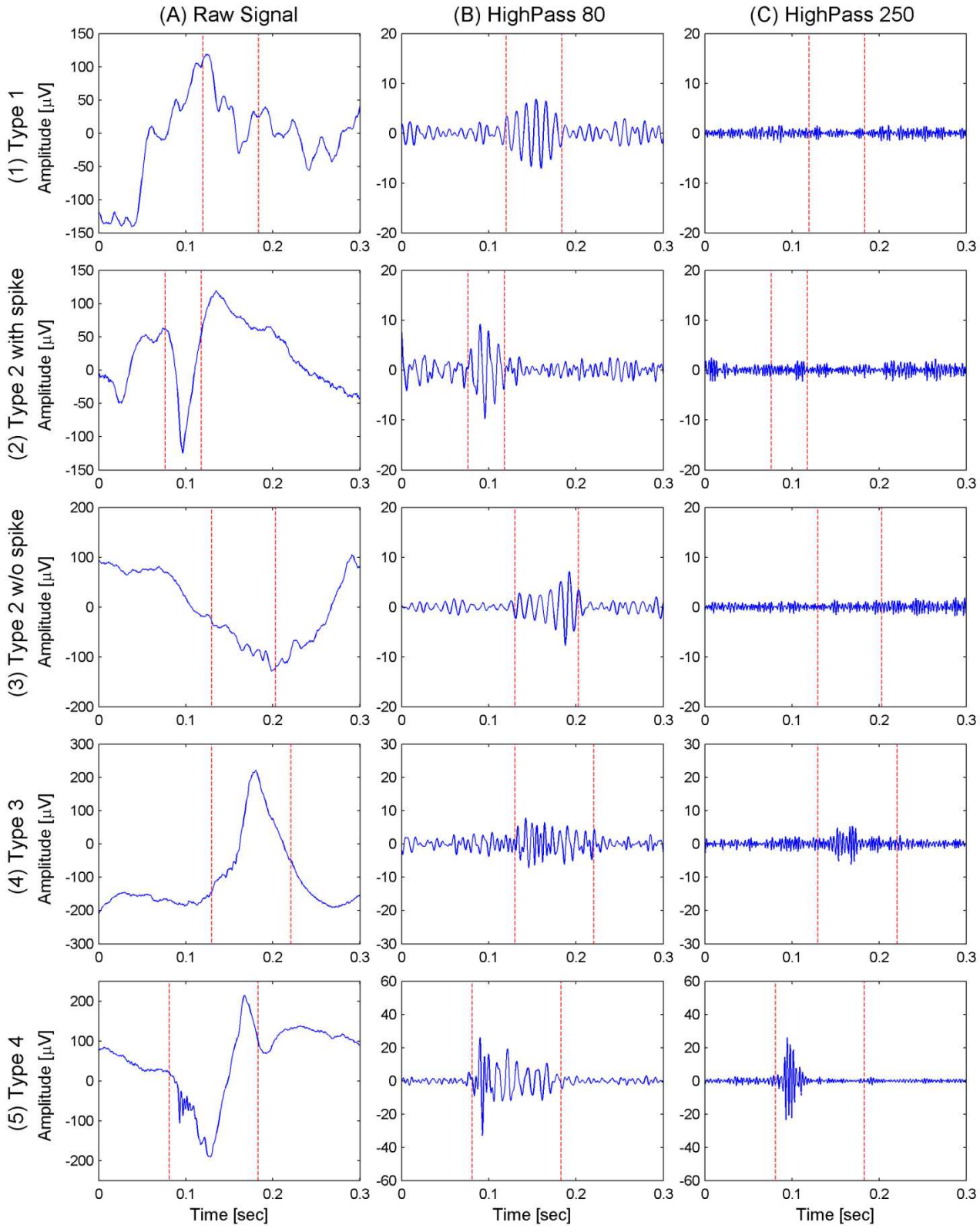
(A) Raw Signal
(B) HighPass 80
(C) HighPass 250
(1) Type 1
(2) Type 2 with spike
(3) Type 2 w/o spike
(4) Type 3
(5) Type 4
Amplitude [μV]
Time [sec]

Figure S2